Modeling the inter-annual variability of ocean circulation and marine ecosystem in the Canary upwelling system

Vladimir Ryabchenko[1], Victor Gorchakov[1], Nikolay Diansky[2], Anton Dvornikov[1], Svetlana Pugalova[1]

[1]St. Petersburg Branch, P.P. Shirshov Institute of Oceanology, Russian Academy of Sciences, 30, Pervaya Liniya, 199053, St.Petersburg, Russia, phone: +7 812 3282729, fax: +7 812 3285759, e-mail: vla-ryabchenko@yandex.ru
[2]Institute of Numerical Mathematics, Russian Academy of Sciences, 8, Gubkina st., 119333, Moscow, Russia, phone: +7 495 9383922, fax: +7 (495)9381821, e-mail: nikolay.diansky@gmail.com

A 3D eco-hydrodynamical model of high resolution is applied to simulate the seasonal and inter-annual variability of ocean circulation and marine ecosystem in the Central-Eastern basin of the North Atlantic (CENA) including the Canary upwelling system. Simulated temperature and salinity fields agree well with satellite and expeditionary observations in the period 1998-2006. According to model results and observations, in the winter period "spots" of maximal phytoplankton biomass are often located in upwelling zones in the open ocean rather than in the coastal upwelling zones. In the summer period, when phytoplankton biomass reaches maximal values, maximums of phytoplankton are located in the coastal upwelling zones. Simulated surface phytoplankton distributions are in qualitative agreement with surface distributions of chlorophyll "a" derived from satellite data. Inter-annual changes in mean annual temperatures averaged over CENA region for the period from 2000 to 2006 amounted to 0.9 °C and 1.0 °C for the model and satellite data, respectively. Similar changes in primary production for the period from 1998 to 2006 amounted to +60, -100 and 50 mgC/(m^2 day) (+6, - 13 and +12% of its mean annual values), respectively, according to the model results, satellite-derived estimate based on the Epply version of standard evaluation method and satellite-derived estimate based on carbon method. Despite the existing quantitative divergences between model results and satellite data, the spatial distributions during the various periods of an annual cycle were similar.

Keywords: circulation, ecosystem, Canary upwelling

1. Introduction

The Central-Eastern basin of the North Atlantic (CENA), including the Canary upwelling system, is among the most productive areas of the ocean, where fishing is intense. It is established that the main physical factors that determine the inter-annual changes in productivity, distribution and abundance of main pelagic fish species in the area, is the intensity of the northeast trade winds and the associated intensity of coastal upwelling, in the presence of meso-scale eddies and the prevalence of South Atlantic central water mass in the subsurface layers of the shelf zone of the North-West Africa [1, 2]. These factors determine the thermal regime in the surface layer of the ocean, and positive and negative anomalies of sea surface temperature in different ways affect the catch of various species of pelagic fish and the level of replenishment of pelagic commercial fish in the CENA [2]. However, the statistical relationships between physical environmental factors (the intensity of upwelling, water temperature, etc.) and fish catching cannot be stable because the influence of physical environmental factors on the replenishment of fish stocks is mediated. Finding of such relationships does not take into account biological factors (phytoplankton and zooplankton) that determine food supply for juvenile fish. In turn, the biomass of phytoplankton and zooplankton depends on the availability of nutrients, light and temperature. Thus, to find a sustainable relationship between fish catching and environmental parameters, it is needed to have an accurate quantitative description of the functioning of the entire pelagic ecosystem in the changing ocean and, above all, to know how physical environmental factors affect the phytoplankton and zooplankton.

This paper is aimed at the study of the impact of seasonal and inter-annual variability of ocean circulation on marine ecosystems in the CENA. For this end, a three-dimensional eco-hydrodynamic model is used. The model is based on coupling of high resolution ocean circulation model developed by the Institute of Numerical Mathematics, Russian Academy of Sciences [3, 4], and ocean ecosystem model developed in [5, 6]. The results to be obtained will be used in future to identify these relationships between fish catching and environmental parameters and their changes due to climate change.

2. The model description

The dynamical block of coupled model developed in [3, 4] is based on the primitive equations of ocean dynamics written using the Boussinesq and hydrostatic approximations in a spherical isobathic coordinate system. Prognostic variables of the model are the horizontal components of velocity, potential temperature and salinity. To calculate the density of seawater, the non-linear equation of state taking into account seawater compressibility and specially designed for ocean circulation models [7] is used. The main feature of the model which distinguishes it from other well-known ocean circulation models is the method of splitting by physical processes at its numerical implementation. The method allows one to effectively implement implicit schemes of integration over time, increase the time step and, thus, improve the efficiency of calculations.

In calculating the transport of the current velocity components, the transport operator is used in a semi-divergent form. The semi-divergent form is well suitable for the transport of current velocity

components and allows the operator to be expanded into non-negative components. The operator is subjected to additional splitting on spatial coordinates that further increases the efficiency of calculation, while conserving the kinetic energy. In contrast to [3, 4], the transport operator for the temperature and salinity, as well as for a passive tracer is used in a divergent form. This conserves the first integral of transported characteristic and does not lead to its dummy sources. In contrast to the divergent form, the semi-divergent form does not con serve the first integral of transported characteristic and can lead to dummy sources of considered characteristics.

A marine ecosystem model developed in [5, 6] is used as a biogeochemical block of the coupled model. The ecosystem model describes the oceanic cycles of nitrogen and carbon and has 12 independent variables: the phytoplankton, zooplankton, bacteria, detritus, nitrate, ammonium, labile dissolved organic carbon, labile dissolved organic nitrogen, and labile dissolved organic carbon, semi-labile dissolved organic nitrogen, semi-labile dissolved organic carbon, and dissolved oxygen.

The equations of the ecosystem model contain 51 parameters. The solution is not very sensitive to the most part of them and/or their values are well known. Some parameters such as mortality rate of phytoplankton and zooplankton, the parameters of grazing of zooplankton, the sinking velocity and the mineralization rate of detritus and others are poorly known, and their values should be determined from sensitivity analysis and comparison of simulation results with observational data. During the expeditions of the Atlantic Institute of Fisheries and Oceanography (AtlantNIRO) in the CENA, carried on regularly since 1994, data on the distribution of chlorophyll, primary production and nutrients were obtained in some areas of this region [8]. However, they do not cover the entire seasonal cycle and the whole area under study and do not contain annual series of measurements in the same location. Therefore, these data can not be used for reliable calibration of the model.

Model calibration was carried out on numerous data obtained in the course of the international program JGOFS (The Joint Global Ocean Flux Study) in the Arabian Sea [9, 10]. The ability to use models tuned to reproduce the evolution of the marine ecosystem in the Arabian Sea, for the CENA is based on the biogeography of the World Ocean using the distribution of planktonic organisms. The whole World Ocean from the point of view of plankton distribution can be divided into three main areas: arctic-boreal, polar and tropical. Plankton of the Arabian Sea and the Canary upwelling region are mainly represented by species of so-called tropical type, which are widespread in the tropical zone of all oceans. Thus, the ecosystems of the Arabian Sea and CENA, located in one and the same latitudinal zone, are rather close and this justifies using the same model in these two areas.

A set of optimal model parameters was obtained from a number of numerical experiments performed with the ecosystem model for the Arabian Sea. Details of these simulations and their comparison with data of American JGOFS expeditions can be found in [4]. These values of parameters were used when performing simulations for the CENA.

The procedure of embedding the ecosystem model into ocean circulation model needs to prescribe somehow z-levels for calculation of photosynthetically active radiation (PAR). The z-levels corresponding σ-levels from ocean circulation model in the point considered are used. The horizontal grid is chosen to be the same as in the model of ocean circulation. Thus, the ecosystem model uses the same 3-dimensional grid as that for temperature and salinity. The simulation of the

ecosystem behavior is performed not in the entire region under study, but only in a part of it (see below). This approach is justified by that the ecosystem model is costly in terms of computing because of a large number of variables.

3. Simulation setup

The above coupled eco-hydrodynamic model was used to simulate oceanic physical and biogeochemical characteristics in the CENA in 2 periods: 1) 1958, and 2) 1998-2006. In carrying out numerical experiments has been allocated two areas: 1) the North and Central Atlantic bounded in the west and east by coasts of continents and in the north and south - by the open boundaries on the parallels of 78° N and 19° S, respectively, and 2) the area of CENA bounded in the north and south by parallels of 15° N and 28° N, in the east – by the African coast and in the west – by the meridian of 18° W (Fig.1). In both areas, the horizontal grid size is 0.25°; the numbers of σ-levels are 27. The equations of the hydrodynamic model are integrated into the first area (for the whole North and Central Atlantic), while ecosystem model equations are solved only for the region of CENA.

The circulation model is driven by momentum, heat and moisture fluxes at the ocean surface and river runoff. These fluxes are calculated using data on atmospheric characteristics prepared within the framework of the program CORE [11] for experiments with ocean-ice models. The database includes data for 1958-2006. A number of atmospheric characteristics (wind speed, atmospheric pressure, air temperature and humidity) have temporal resolution 6h, the sea surface fluxes of absorbed short-wave radiation and total long-wave radiation are given as mean daily values, the rate of precipitation - as monthly mean values, the river discharge - as the mean annual values. Wind stress and fluxes of sensible and latent heat are calculated from the known bulk-formulas. The total heat flux at the ocean surface is calculated from the equation of the heat budget of ocean surface using short-wave and long-wave radiation from [11]. The total flux of moisture (precipitation minus evaporation) is determined according to the rate of precipitation from [11] and the evaporation rate calculated using the model ocean surface temperature. At open boundaries of the region 1 (the North and Central Atlantic) temperature and salinity are prescribed from the archive [12] (mean monthly climatic data with a space resolution of 0.25°). The discharge of major rivers is parameterized through the precipitation near river mouths as is sometimes done in climate models (see [13]).

Calculations of ecosystem variables were carried out by splitting in two stages. First, at each time step, the local problem for the CENA region is solved without the allowance for advective and diffusive transports (both horizontal and vertical ones). The needed temperature and salinity values at grid nodes were taken from the solution of the hydrodynamic model in the previous time step. The diurnal variation of the absorbed solar radiation (as well as PAR) at the ocean surface was restored using its average daily values from the archive CORE [11]. In the second stage, the hydrodynamic characteristics (current velocity, temperature, salinity) for the region 1 are calculated, and obtained components of current velocity are used to calculate the transport (as advection and diffusion) of ecosystem characteristics, considered as passive tracers, in the CENA region. At the open boundaries, nitrate and oxygen concentrations are prescribed from of the Levitus' archives [14]

and [15], respectively; for all other variables, radiation condition is used for outflow currents and no-flux condition is specified for inflow currents. Note that the gravitational sinking of detritus was taken into account in the second stage by introducing a total transport rate, defined as the sum of the vertical component of the current velocity and the velocity of detritus sinking.

In the case of 1958, the initial conditions were specified as mean January distributions of nitrate and dissolved oxygen from the Levitus' archive, linearly interpolated to the computational grid. For other ecosystem variables some uniform distributions were set, where the values of semi-labile dissolved organic carbon and dissolved organic nitrogen were respectively 20 and 10 mmol m^{-3}, and all remaining variables were assigned some small values. The initial distribution of thermo-hydrodynamic characteristics was taken from a run on the hydrodynamic model, performed for region 1 for a period of 14 years. The run of the coupled model lasted 2 years, starting from 1 January 1958, with preservation of external atmospheric forcing of 1958 for the second year of the run.

In the run for 1998-2006, the hydrodynamical model was integrated from 1958 and the coupled model started from 1998. The initial conditions for ecosystem variables were taken from the solution for 1958, at 24:00 31 December.

4. Results

4.1. Seasonal variations (the run for 1958)

Below we discuss the results of the second year of simulation, when the upper mixed layer of the ocean reached a quasi-equilibrium regime. As seen from the model surface distribution of nitrate and phytoplankton of 15 January (Fig. 2, 3b), the maximum surface concentrations of nitrates (up to 22 mmol N m^{-3}) in winter occur in coastal upwelling areas to the south of Cap Blanc and near Cape Timiris (19° N). The solution is qualitatively consistent with the climatic data on the concentration of nitrates (Fig.4). With increasing depth, nitrate concentrations are increasing, its horizontal distribution near the surface and at depth of 50 m are practically the same everywhere except the southern part (south of 18 ° N) of the model domain, which indicates the existence of well-mixed layer with a thickness not less than 50 m (Fig.2a, 2b). Distribution of nitrate at 100 m (Fig.2c) is characterized by zones of high and low concentrations. It is noteworthy that the maximum model nitrate concentration at the depth of 100 m is located in the southern part of the model domain, south of 22 ° N, that agrees well with climatic mean monthly nitrate distribution (Fig.4c). This leads to the maximum surface concentrations of nitrates in the same part of the study area (south of Cap Blanc), while the maximal coastal upwelling velocity occurs north of Cap Blanc between 25 ° and 28° N (Fig. 3a).

In accordance with the distribution of nitrate, phytoplankton and zooplankton are also concentrated in the southern part of the model domain, where, in addition to the maximum mineral supply, higher temperature promotes a more intensive production (Fig. 3b, 3c). However, the maximum biomasses of phytoplankton and zooplankton are often located not in areas of coastal upwelling, but farther out to sea, and in general do not coincide with the zones of maximum nitrate concentrations. Rather, the distribution of plankton is determined by the characteristics of the

surface circulation (Fig. 3a). For example, spot of increased phytoplankton biomass having the center in (17°N, 19.5° W) is localized in the open ocean in the upwelling zone (Fig. 3a, 3b). With increasing of depth the phytoplankton biomass decreases, so that at 100 m its values are an order of magnitude smaller than at the surface. Interestingly, the "spots" of increased phytoplankton biomass at the ocean surface in the southern part of the model domain are replaced by "spots" of lowered phytoplankton biomass at the horizon 50m, which are localized almost under "spots" of increased phytoplankton biomass. This drop in phytoplankton is most likely caused by the effect of self-shadowing: in places of high phytoplankton biomass PAR intensity markedly decreases with depth that leads to a strong decrease in primary production and phytoplankton biomass on the horizon 50m.

In April, in contrast to January, the region of increased nitrate concentrations is located north of Cap Blanc; the surface nitrate concentration is much lower. The distribution of phytoplankton has pronounced peaks and is close to uniform distribution with a slight increase in biomass from the north-eastern corner of the model domain to the southwest one, while the zooplankton biomass is approximately 2 times higher than in January. This indicates that, on the one hand, the nitrates are largely used by phytoplankton, and phytoplankton, in turn, eaten by zooplankton. The influence of surface currents on the distribution of phytoplankton is manifested in the existence of narrow "tongues" of increased biomass, elongated almost perpendicular to the shoreline at latitudes 33, 29 and 21° N, as well as in the existence of low phytoplankton biomass off the coast of Africa at 16-17° N. Nitrate concentrations increase with depth, while maintaining the basic features of surface distribution. The maximum biomass of phytoplankton at the depth of 50m occurs in the zone of coastal upwelling to the north of Cap Blanc, as well as near the western boundary of the model domain at 18° N.

In July compared to January, the regions of increased nitrate concentrations in the coastal zone are distributed in different way. Although to the south of Cap Blanc, there are still regions of strong upwelling, but with lower concentrations of nitrates, there are also strong upwelling regions to north of Cap Blanc (Fig. 5a). With the depth, the distribution of nitrate varies considerably already at the horizon 50 m (Fig. 5b, 5c), indicating that in summer the mixed layer thickness is less than 50m. When comparing the calculated distributions of nitrate to climatic ones shown in Fig. 7, attention is drawn to the presence in the solution of the two spots of increased nitrate concentrations in the upper ocean (to the north of Cap Blanc and Cape Timiris), which is absent in the data. According to these data, the two spots of high nitrate concentrations occur only at depths exceeding 100 m. This may be due to the fact that the model overestimates the vertical advective transport of nitrate to the surface from depths exceeding 100 m. Most likely, the same factor causes a slight increase in the calculated values of nitrate concentrations reaching 14 mmol N/m3 in the spots. Another possible reason for this marked discrepancy may be due to the fact that the results of the solution on the grid with a resolution of 0.25 degrees with the atmospheric forcing, corresponding to an individual year, compared with those from climate archive on the one-degree grid.

Phytoplankton biomass in July is generally higher than in January, especially in the northern part of the model domain and more evenly distributed, with maximum values are concentrated mainly near the coast in areas of upwelling (Fig.6b). Zooplankton is also markedly higher than in January (Cf. Fig.3c and Fig.6c). Such distribution of biomass of phytoplankton and zooplankton are

consistent with the pattern of surface currents, according to which the Canary Current in July is located much closer to the coast than in January (Fig.6a). The thickness of the mixed layer in July is less than in January that is confirmed by the distribution of phytoplankton at a depth of 50m, where the values biomass fell to 0.2 mmol N m^{-3}. In other words, the phytoplankton in July is concentrated in the upper mixed layer and almost absent in the seasonal thermocline.

In November, the surface distribution of nitrate is similar to that in July, differing more pronounced coastal zone of increased nitrate concentrations in the northern part of the model domain and to the south of Cap Blanc. Horizontal distribution of nitrate concentration at the surface and at depths of 50 m are very close everywhere except the southern part (south of 18 ° N) of the model domain, which indicates on the existence of the mixed layer thickness of about 50m. However, the surface distributions of phytoplankton and zooplankton are strongly different from their distributions in July and are similar to the April distributions without a pronounced maximum. As in April, the biomass of phytoplankton and zooplankton is increased from north-eastern corner of the model domain to the southwest.

4.2. Inter-annual variations (the run for 1998-2006)

According to the model results, the sea surface temperature (SST) averaged over the study area experiences seasonal fluctuations with double-amplitude peak of about 6 ºC and a maximum in the second half of September - the first half of October (Fig. 8). The calculated values of SST are in good agreement with available satellite data for the period from 2000 to 2006 (http://podaac.jpl.nasa.gov/datasetlist/): calculated temperature was slightly below the observed but not more than 1.5 °C. According to the model results and satellite measurements, changes in mean annual temperature for the period from 2000 to 2006 are of 0.9 and 1.0 ºC, respectively.

Comparison with data on temperature and salinity from AtlantNIRO expeditions [see 8 and http://www.atlantniro.ru/] showed that in the spring of 1998 (February 26 - April 5) modeled distributions of temperature and salinity at the horizon z = 10m are in a qualitative agreement with the observed distributions, although underestimate observed temperature and salinity about 2 °C and 0.5 ‰, respectively (Fig. 9). Temporal (inter-annual and seasonal) changes in temperature and salinity are also well simulated. In particular, in the spring of 1999 (April 3-May 1, that is, in a later period than in 1998) in the northern part of the study area, temperature and salinity were 2 ºC and 0.5 ‰, respectively, lower than in 1998. The main difference between the summer SST and its winter and spring distributions is a significant increase in temperature in the southern part of the CENA, this increase in 1999 being significantly (3°C) higher than in 1998.

Seasonal changes in the calculated chlorophyll "a" concentration at two typical locations of the CENA were small: during the annual cycle, they changed not more than 3-fold (Fig. 10). The values of chlorophyll "a" concentration measured in AtlantNIRO expeditions in 1998 at the same locations were higher than calculated in 2-5 times. Satellite-based chlorophyll concentrations taken from [16] in the same locations were turned out to be 3-fold higher than the AtlantNIRO data (Fig. 10b, 10c). However, a similar comparison of model and observed values of chlorophyll concentration in 1999 (Fig.11a) is indicative of their reasonable agreement. We also note that the observations in nearby locations in near time instants are often different from each other in several

times, indicating a high spatial and temporal variability of chlorophyll concentration. Apparently, this is one of the reasons for the marked discrepancies between the model and AtlantNIRO data as well as between the AtlantNIRO and satellite-based data. Other reasons for these discrepancies could be: 1) the proximity of the coast, distorting the signal and estimates of chlorophyll in the remote sensing data, 2) conversion of the biomass of phytoplankton to the chlorophyll concentration using a constant conversion factor, while the ratio of phytoplankton biomass and chlorophyll concentration is a complicated function of the PAR, the concentration of limiting nutrient and water temperature.

Despite significant quantitative differences between calculated and satellite-based surface chlorophyll concentrations at some locations, their spatial distributions at different times of the annual cycle were rather similar. As an example, Fig. 12 presents the calculated surface distribution of phytoplankton biomass and satellite-based concentrations of chlorophyll "a" in early April 1998. As can be seen, the model correctly reproduces the maximum values of chlorophyll in the narrow coastal upwelling zone between 16 and 25.5 ° N, west elongated zone of high chlorophyll concentrations between 18 and 21 ° N, low concentrations in other parts of the study area. However, the model distribution has been much smoother than the observed. This may be due to either insufficient high horizontal resolution of the model or an overestimation of the coefficient of horizontal turbulent diffusion.

Comparison of calculated and satellite-derived primary production taken from [16] (Fig. 13) shows that the model overestimates the average level of primary production. It correctly reproduces the double-amplitude peak of the inner-annual oscillations and the instant of minimum value, but results in a delay of instant when maximum value is reached. Model estimates of primary production overestimate 30-40% and more than 2-fold satellite-derived estimates obtained using the method of Eppley and carbon method, respectively. In present, the reasons for this overestimation and the delay of timing of maximum primary production are unknown. In the latter case as one of the possible causes may be the excess of nitrates in the oceanic upper mixed layer. This leads to the fact that they no longer limit the phytoplankton production during photosynthesis. In this case, the dominant influence on primary production provides the water temperature, the maximum of which, also as primary production maximum, occurs at the end of September (Cf. Figs.7 and 13). Inter-annual changes in mean annual values of primary production in the period 1998 to 2006 are 60, 100 and 50 mg C / (m^2 day) (+6, - 13 and +12% of the average annual values), according to the model results, Eppley' standard method and carbon method, respectively.

5. Concluding remarks

Thus, the comparison of model solution with the observational data shows that the model correctly both qualitatively and quantitatively simulates the seasonal and inter-annual variability of physical characteristics (first of all, temperature and salinity) in the CENA. This is not so for the simulation of the variability of biogeochemical variables: in some cases there are significant differences between the model and satellite-derived data. Moreover, there are also significant differences between satellite and expeditionary data. The reasons for these discrepancies can be clarified by a careful analysis of the results of calculations and study the sensitivity of solution to

poorly known parameters such as mortality rate of phytoplankton and zooplankton, the parameters of grazing and excretion of zooplankton, the sinking velocity and the rate of mineralization of detritus, etc.

Acknowledgements. The authors were supported by the Russian Foundation for Basic Research, grant 09-05-00668-a.

References

1. Malinin V.P., Chernyshkov P.P., Gordeeva S.M. 2002. Canary upwelling: a large-scale climate variability and prediction of water temperature. St.Petersburg, Gidrometeoizdat, 154p. (In Russian)

2. Sirota A.M. 2003.The structure and water dynamics in the Canary upwelling region, and status of populations of pelagic fish. *PhD thesis.* Kaliningrad, 182p. (In Russian)

3. Alekseev V.V., Zalesny V.B. 1993. A numerical model of large-scale ocean dynamics. *In: Numerical processes and systems.* Ed. G.I. Marchuk. Issue 10. Moscow, Nauka, 232-252 (in Russian).

4. Diansky N.A., Bagno A.V., Zalesny V.B. 2002. Sigma-model of the global ocean circulation and its sensitivity to variations in wind stress. *Izvestiya, Atmospheric and Oceanic Physics,* 38, No 4, 537-556. (In Russian)

5. Ryabchenko V.A., Gorchakov V.A., Fasham M.J.R. 1998. Seasonal dynamics and biological productivity in the Arabian Sea euphotic zone as simulated by a three-dimensional ecosystem model. *Global Biogeochemical Cycles,* V.12, 501–530.

6. Anderson T.R., Ryabchenko V. A., Fasham M. J., Gorchakov V. A. 2007. Denitrification in the Arabian Sea: A 3D ecosystem modeling study. *Deep-Sea Research I*, 54, 2082-2119.

7. Bryden D., San S., Bleck R. 1999. A new approximation of the equation of state for seawater, suitable for numerical ocean models. *J. Geoph. Res.* V.104, No.C1, 1537-1540.

8. Commercial -oceanographic studies in the Atlantic Ocean and the South Pacific (according to the researches of AtlantNIRO and Zaprybpromrazvedki). 2002. Ed. V.N. Yakovlev. Kaliningrad, AtlantNIRO, 248p. (In Russian)

9. Lee C., Murray, D.W., Barber, R.T. et al. 1998. Particulate organic carbon fluxes: compilation of results from the 1995 US JGOFS Arabian Sea process study. *Deep-Sea Research II*, V. 45, P. 2489–2501.

10. Sarma V.V.S.S., Swathi P.S., Kumar M.D. et al. 2003. Carbon budget in the eastern and central Arabian Sea: An Indian JGOFS synthesis. *Global Biogeochemical Cycles,* V.17 (4), 1102, doi:10.1029/2002/GB001978.

11. Large, W. G., Yager S. G. 2004: Diurnal to Decadal Global Forcing for Ocean and Sea-Ice Models: The Data Sets and Flux Climatologies. 113 pp. Climate and Global Dynamics Division. National Center for Atmospheric Research. Boulder, Colorado.

12. Boyer, T.P., Levitus S. 1997. Objective analysis of temperature and salinity for the world ocean on a 1/4 degree grid. NOAA Atlas NESDIS 11.

13. Moshonkin, S.N., Diansky N.A., Gusev A.V. 2007. Effect of interaction between the Atlantic and Arctic Oceans on the Gulf Stream. Oceanology. V. 47, No. 2, P.197-210 (In Russian).

14. Conkright M. E., Boyer T. P., Antonov J. I. et al. 2002. NOAA Atlas NESDIS 46 WORLD OCEAN DATABASE 2001. Volume 5: Temporal distribution of nutrient profiles. Edited by S. Levitus. Washington, D.C.: U.S. Gov. Printing Office, 286p.

15. Locarnini R. A., Conkright M. E., Antonov J. I. et al. 2002. NOAA Atlas NESDIS 45 WORLD OCEAN DATABASE 2001 Volume 4: Temporal distribution of temperature, salinity and oxygen profiles. Washington, D.C.: U.S. Gov. Printing Office, 332p.

16. *Ocean Productivity site* : http://www.science.oregonstate.edu/ocean.productivity/index.php/.

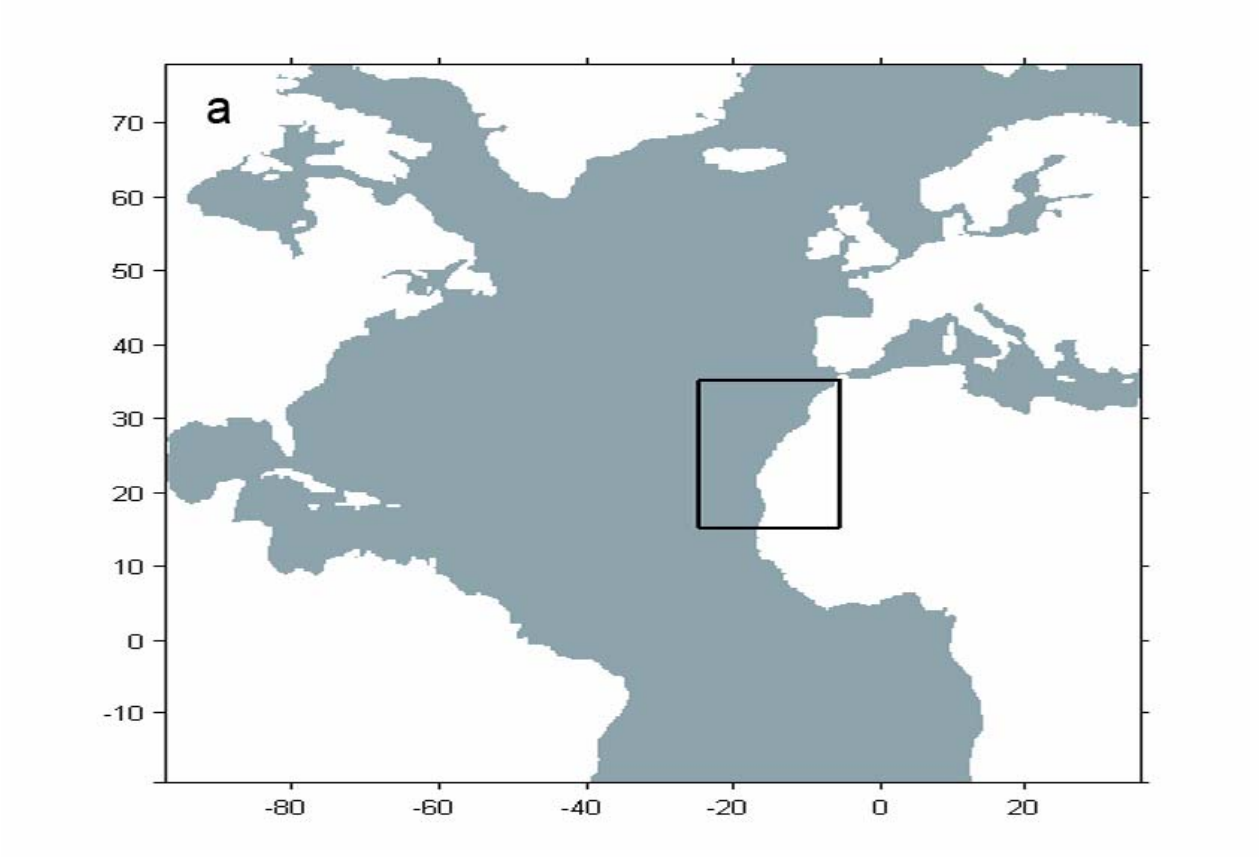

Fig.1. The domain of integration of equations of the hydrodynamic model (region 1) and the CENA region, where the equations of ecosystem model are solved (part of the sea within the rectangle).

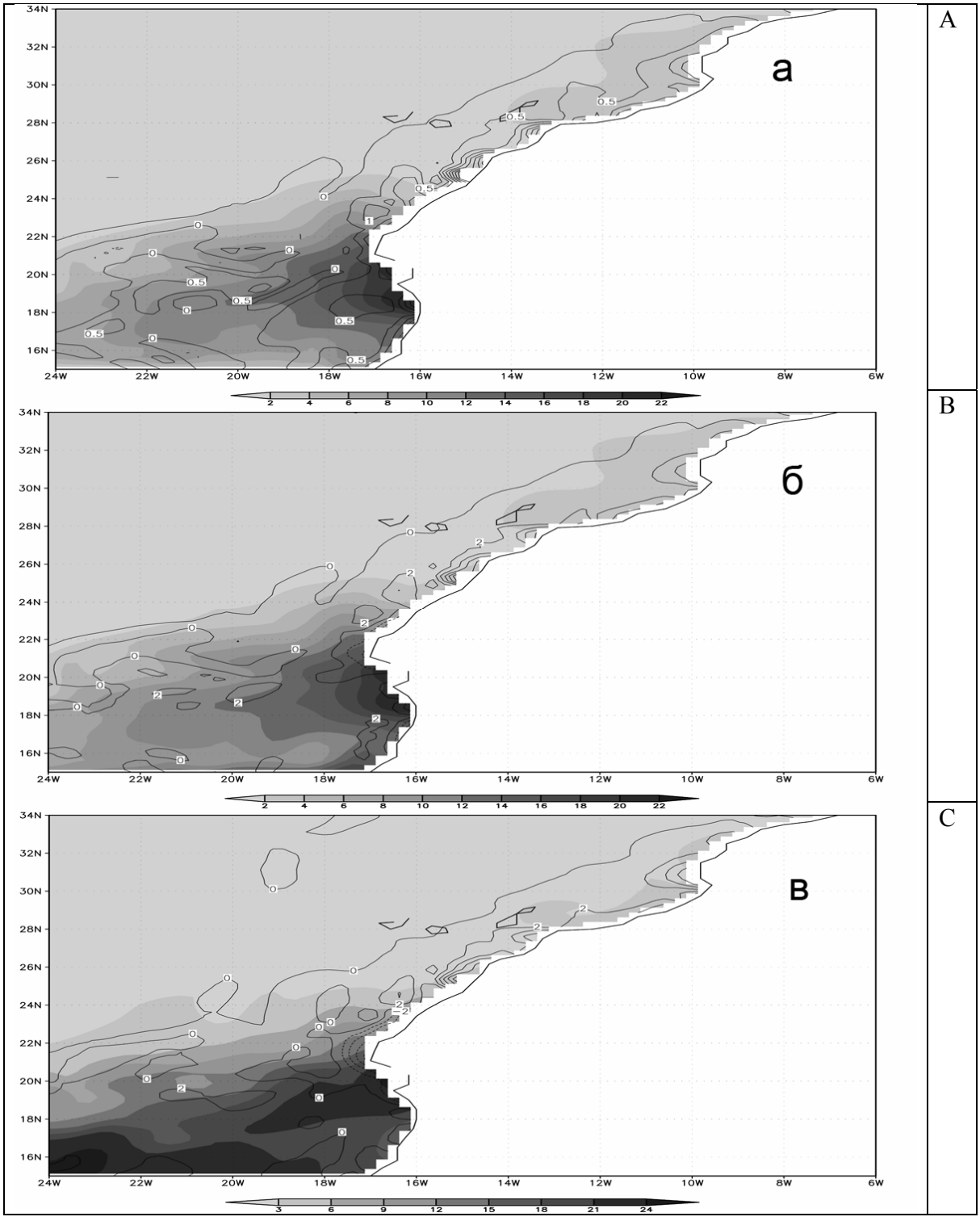

Fig.2. Distributions of nitrate (mmol N m^{-3}) and the vertical component of the current velocity (isolines of w $\times 10^3$ cm s^{-1}) at levels 10, 50 and 100 m (a, b and c, respectively) in the CENA on 15 January.

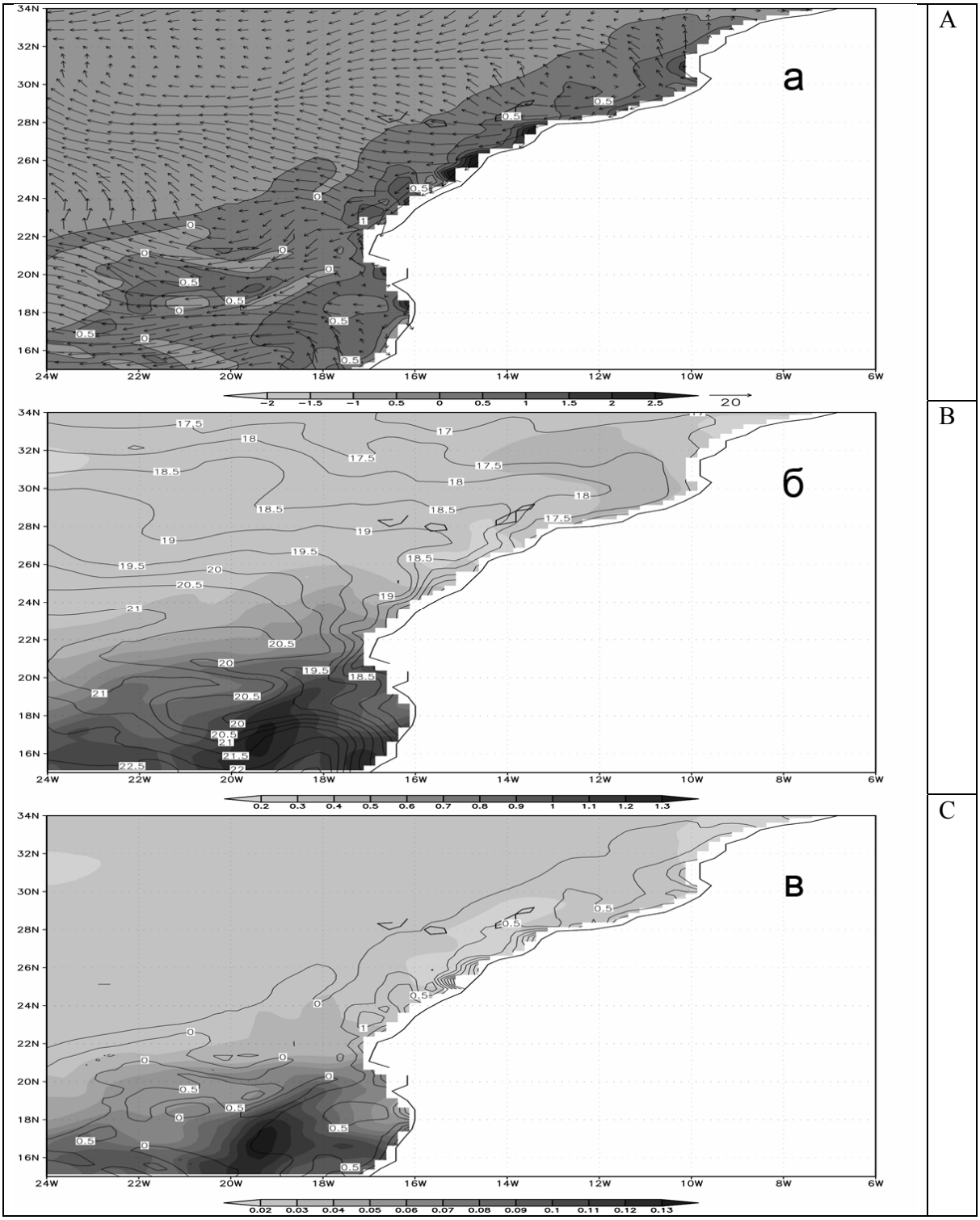

Fig.3. Distributions of horizontal (cm s^{-1}) and vertical (isolines of w $\times 10^3$ cm s^{-1}) components of the current velocity (a); phytoplankton (mmol N m^{-3}) and temperature (isolines, ^oC) (b); zooplankton (mmol N m^{-3}) and the vertical component of the current velocity (isolines of w $\times$ 10^3 cm s^{-1}) (c) in the ocean surface layer in the CENA on 15 January.

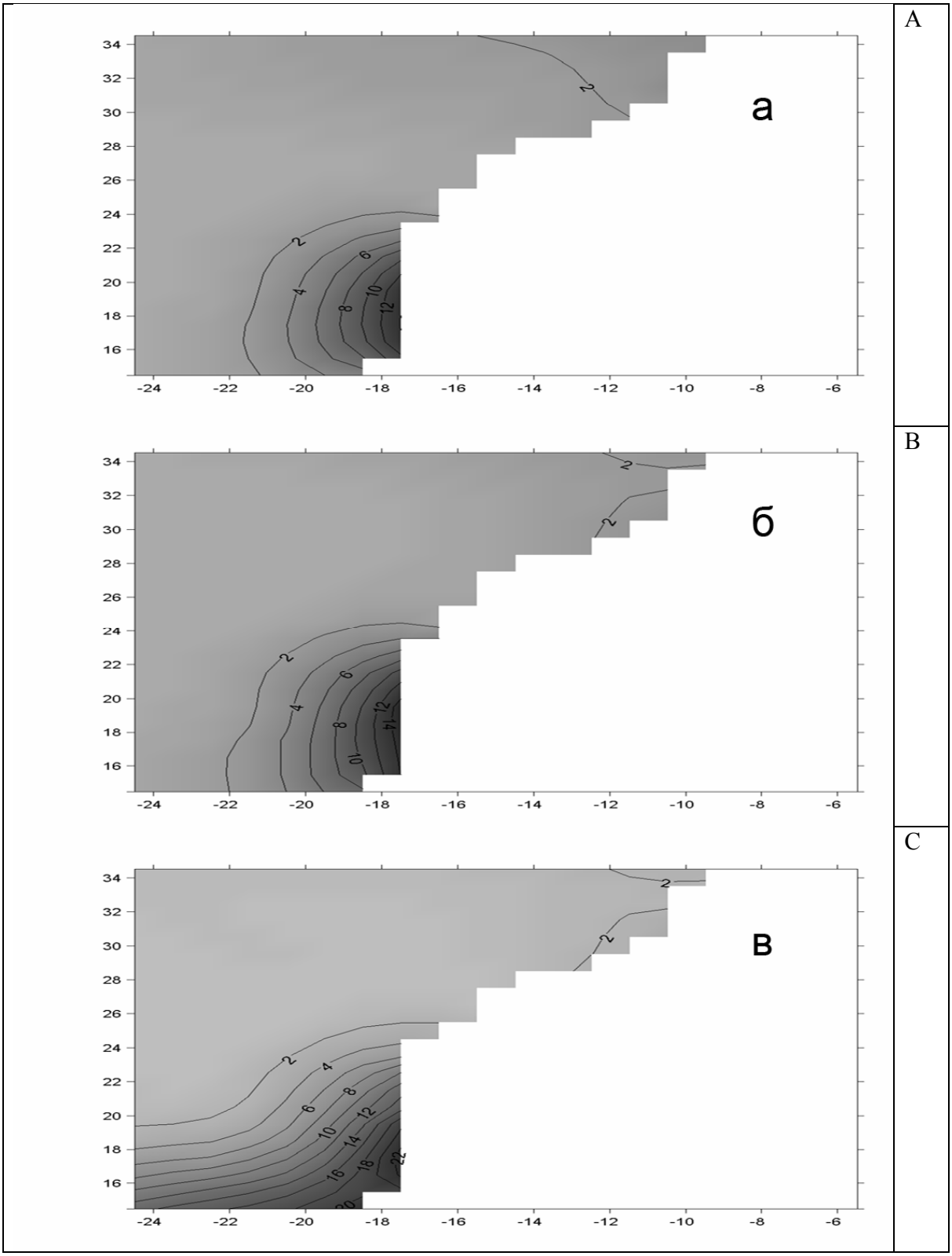

Fig.4. Mean monthly nitrate distributions (mmol N m^{-3}) in January at 10, 50 and 100 m (a, b and c, respectively) in the CENA, according to [14].

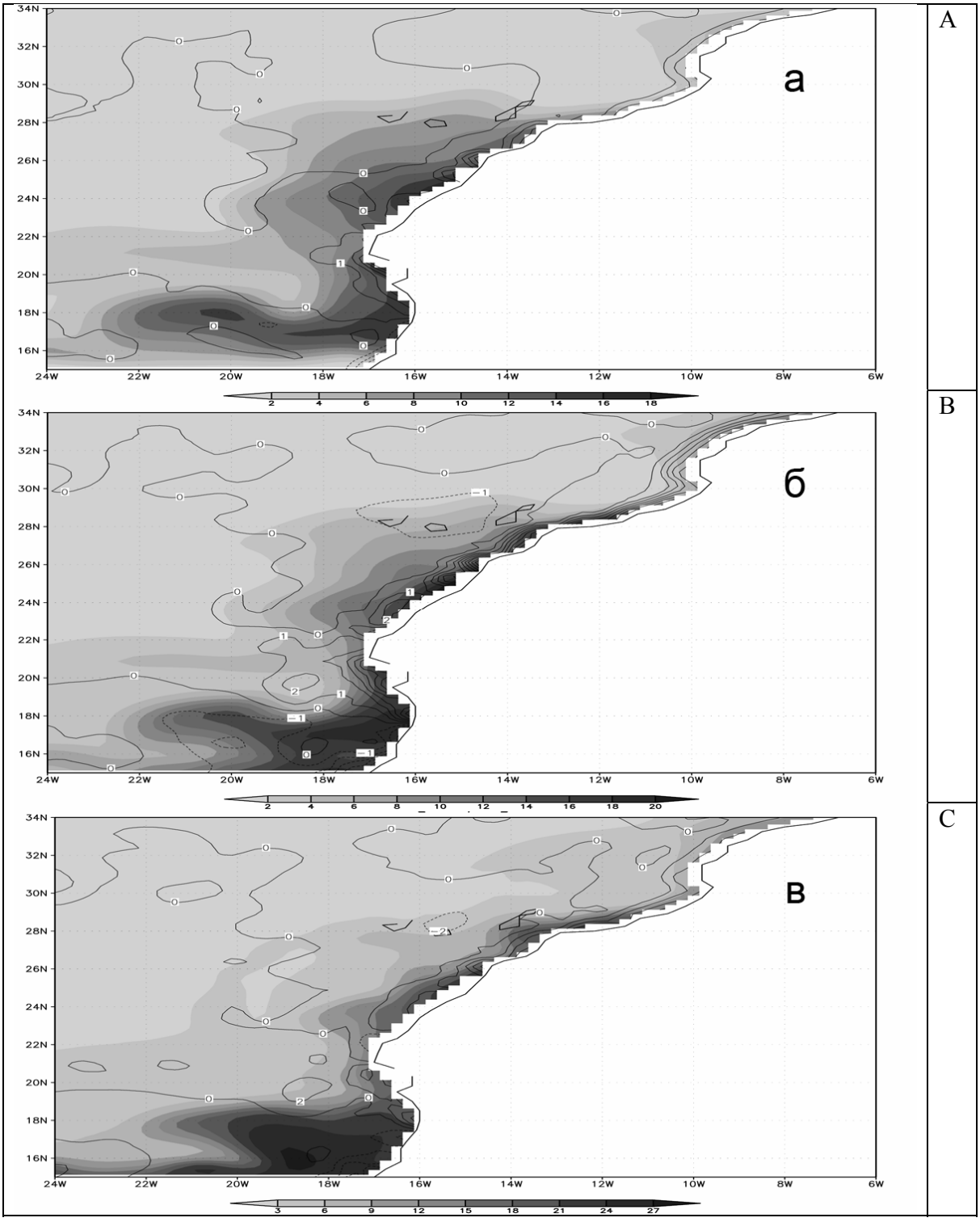

Fig.5. Distributions of nitrate (mmol N m^{-3}) and the vertical component of the current velocity (isolines of w $\times 10^3$ cm s^{-1}) at levels 10, 50 and 100 m (a, b and c, respectively) in the CENA on 15 July.

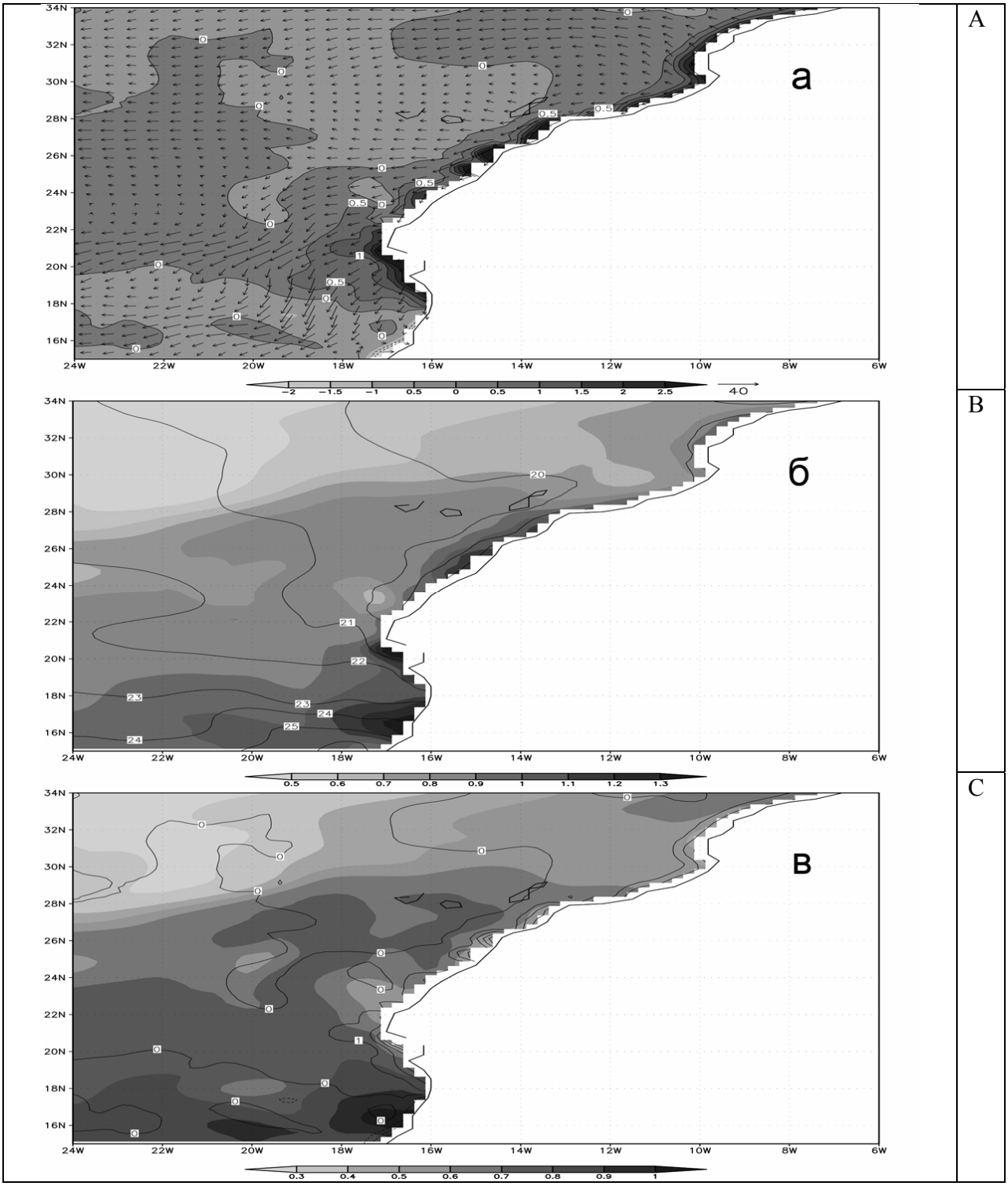

Fig.6. Distributions of horizontal (cm s^{-1}) and vertical (isolines of w $\times 10^3$ cm s^{-1}) components of the current velocity (a); phytoplankton (mmol N m^{-3}) and temperature (isolines, ^oC) (b); zooplankton (mmol N m^{-3}) and the vertical component of the current velocity (isolines of w $\times$ 10^3 cm s^{-1}) (c) in the ocean surface layer in the CENA on 15 July.

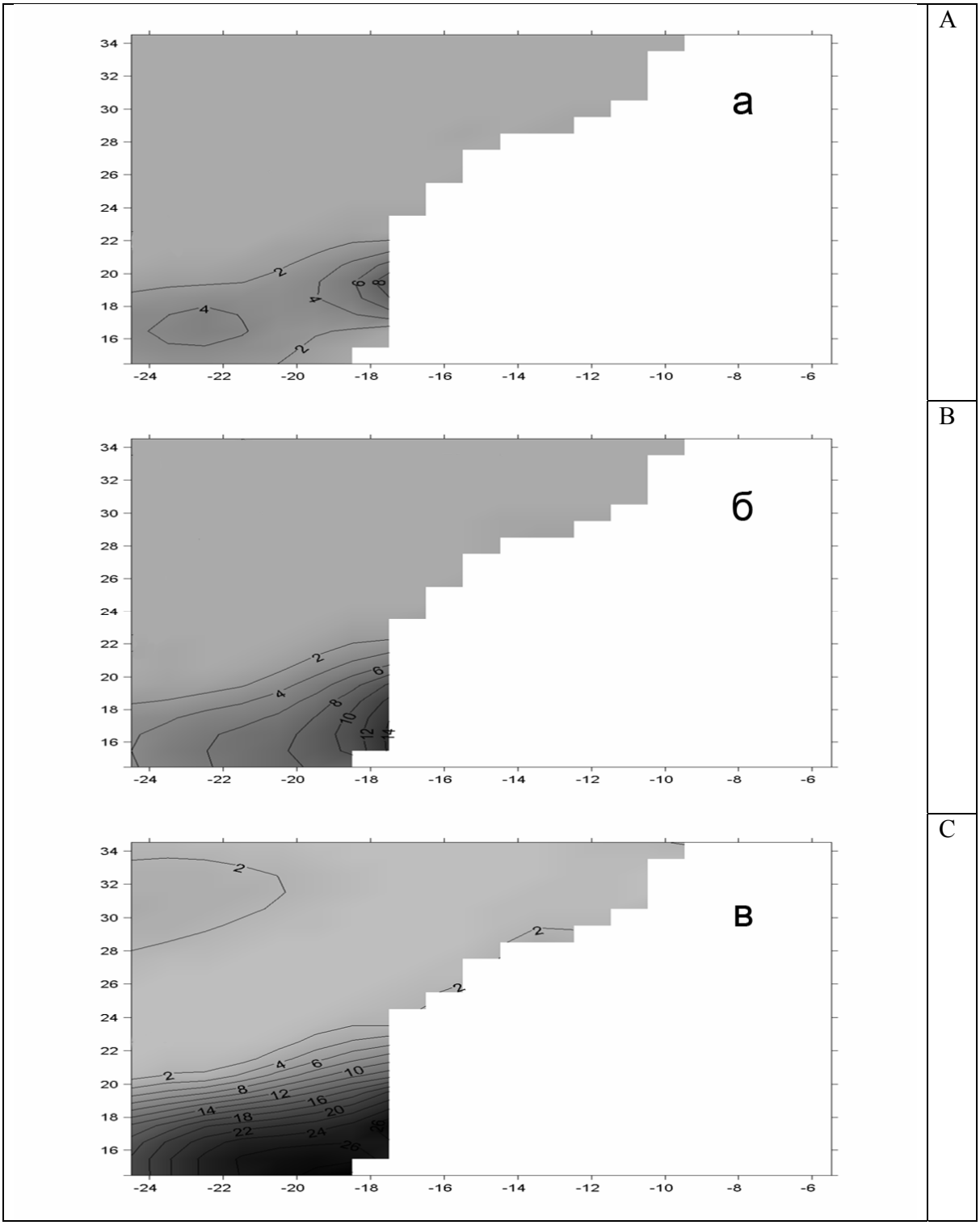

Fig.7. Mean monthly nitrate distributions (mmol N m^{-3}) in July at 10, 50 and 100 m (a, b and c, respectively) in the CENA, according to [14].

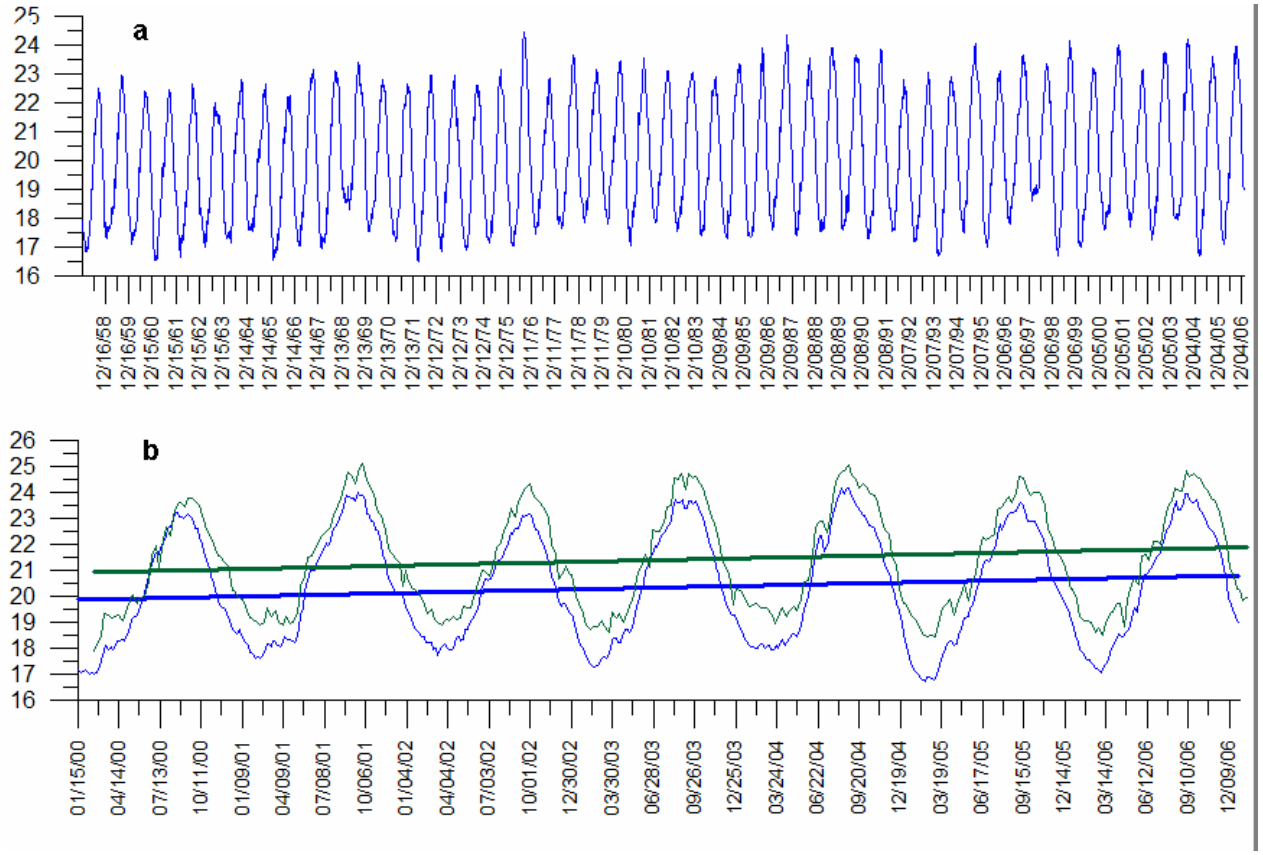

Fig.8. Temporal evolution of area-averaged sea surface temperature (ºC): (a) the model results for the period from 1958 to 2006, (b) the model results (blue lines) and MODIS data (green lines) for the period from 2000 to 2006. Straight lines are linear trends in temperature variations.

Temperature distribution (26 february 1998 - 5 april 1998)

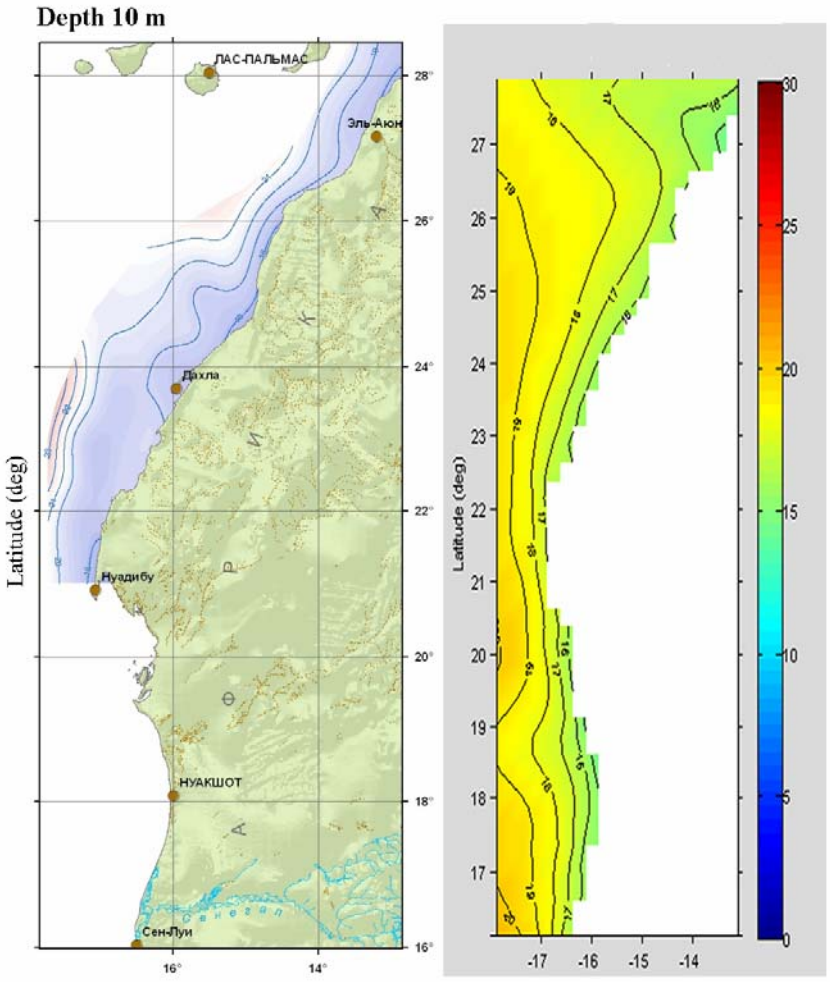

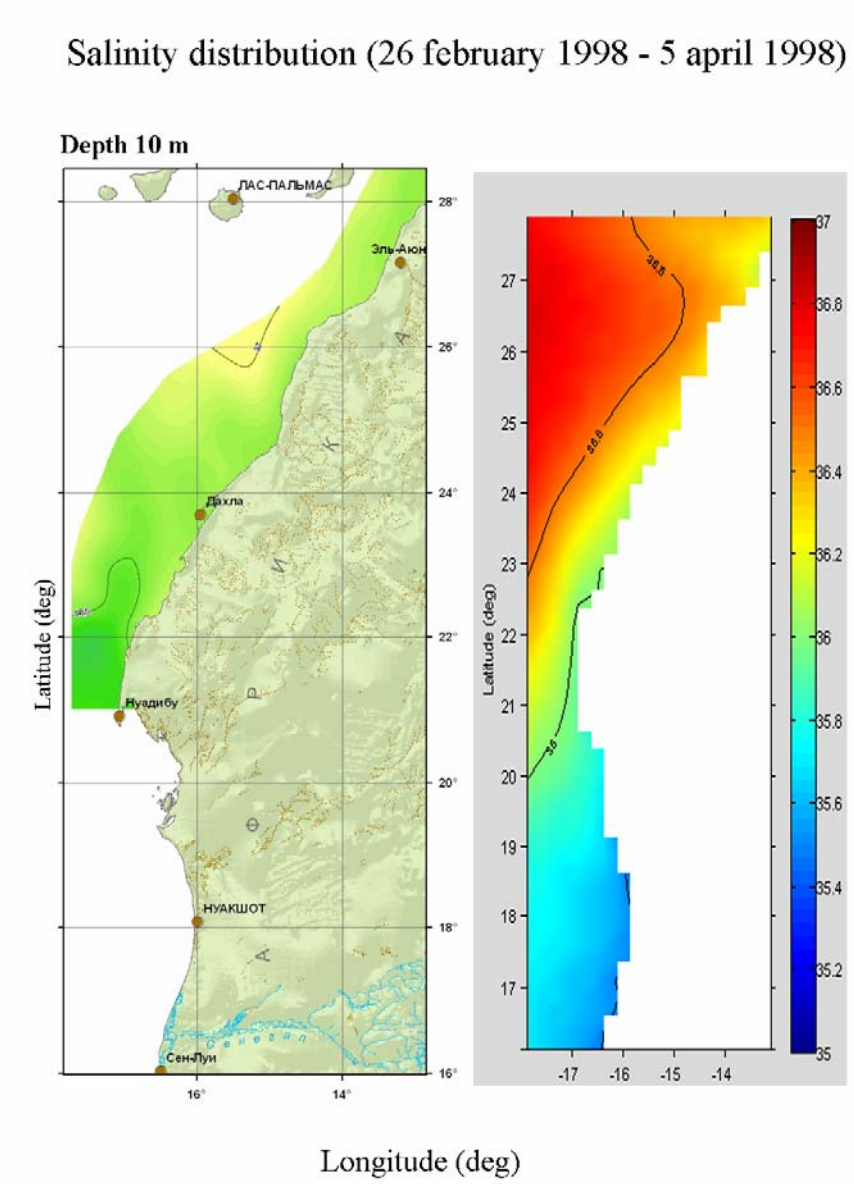

Fig.9. The average (over the period of expeditionary measurements) distributions of temperature and salinity at the horizon z = 10 m in the CENA in spring 1998 according to AtlantNIRO data (left fragments) and the model results (right fragments).

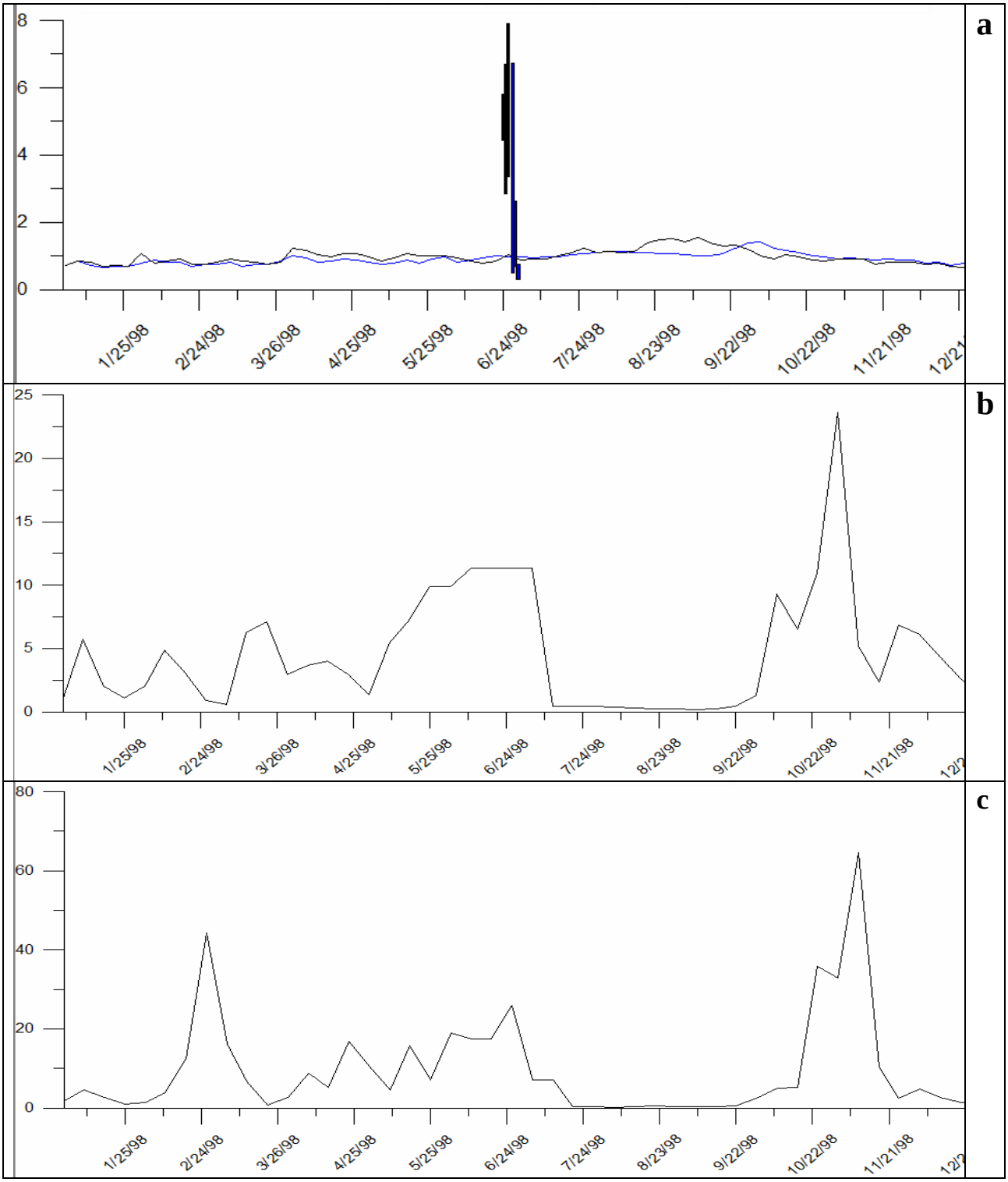

Fig.10. Seasonal variability of sea surface concentration of chlorophyll "a" (mg/m3) at two locations: (19 º N, 17 º W) and (17 º N, 17 º W) in 1998.

Fragment a: black and blue curves are calculation results respectively in the first and second points; vertical lines of the corresponding color are AtlantNIRO data in the close vicinity of these points. Each vertical line shows the limits of the measured concentrations in the layer (0-10m). Fragments b and c: SeaWiFS data (http://seawifs.gsfc.nasa.gov/) at locations (19 º N, 17 º W) and (17 º N, 17 º W), respectively.

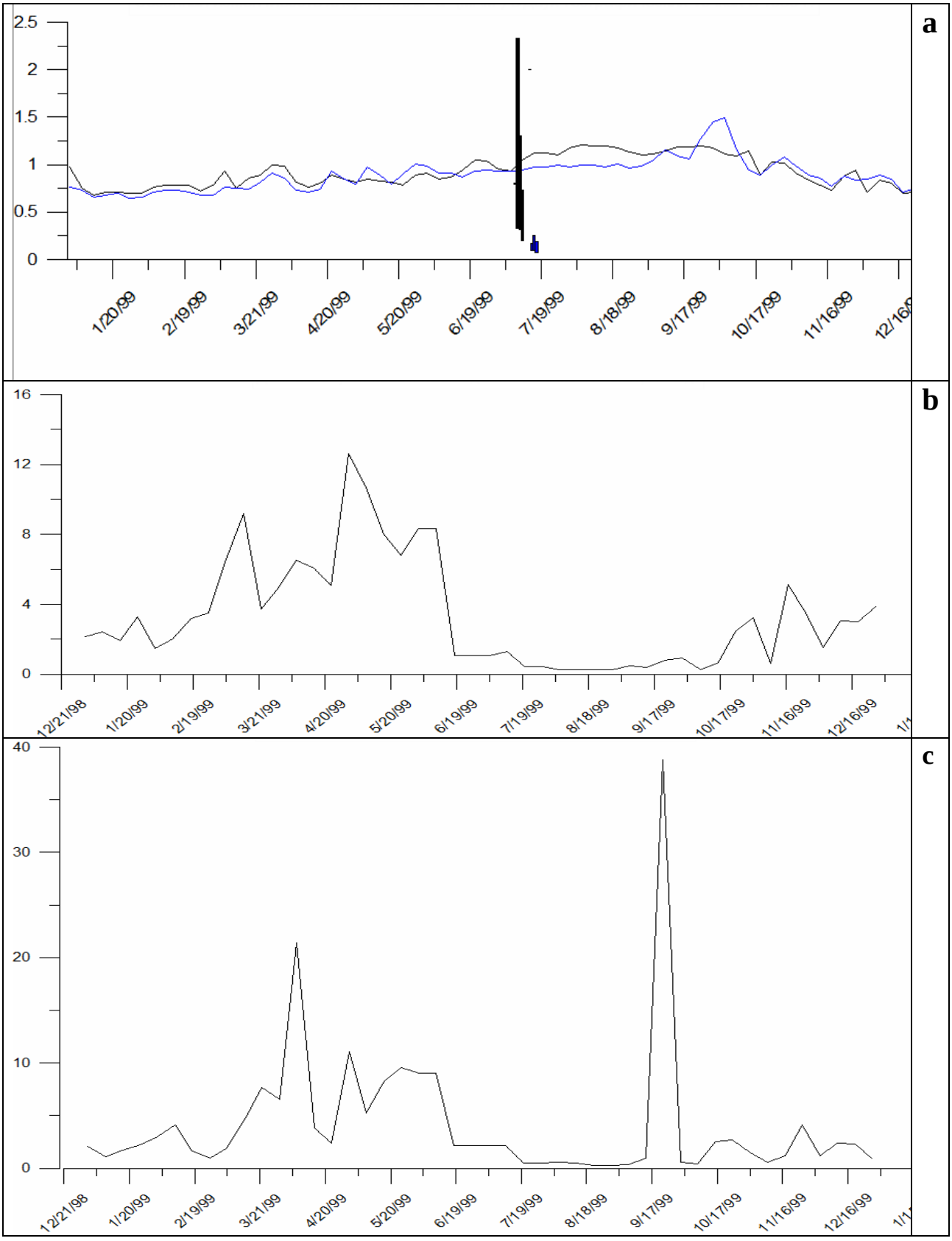

Fig. 11. Seasonal variability of sea surface concentrations of chlorophyll "a" (mg/m3) at the same locations as in Fig. 10 in 1999. See legend in Fig. 10.

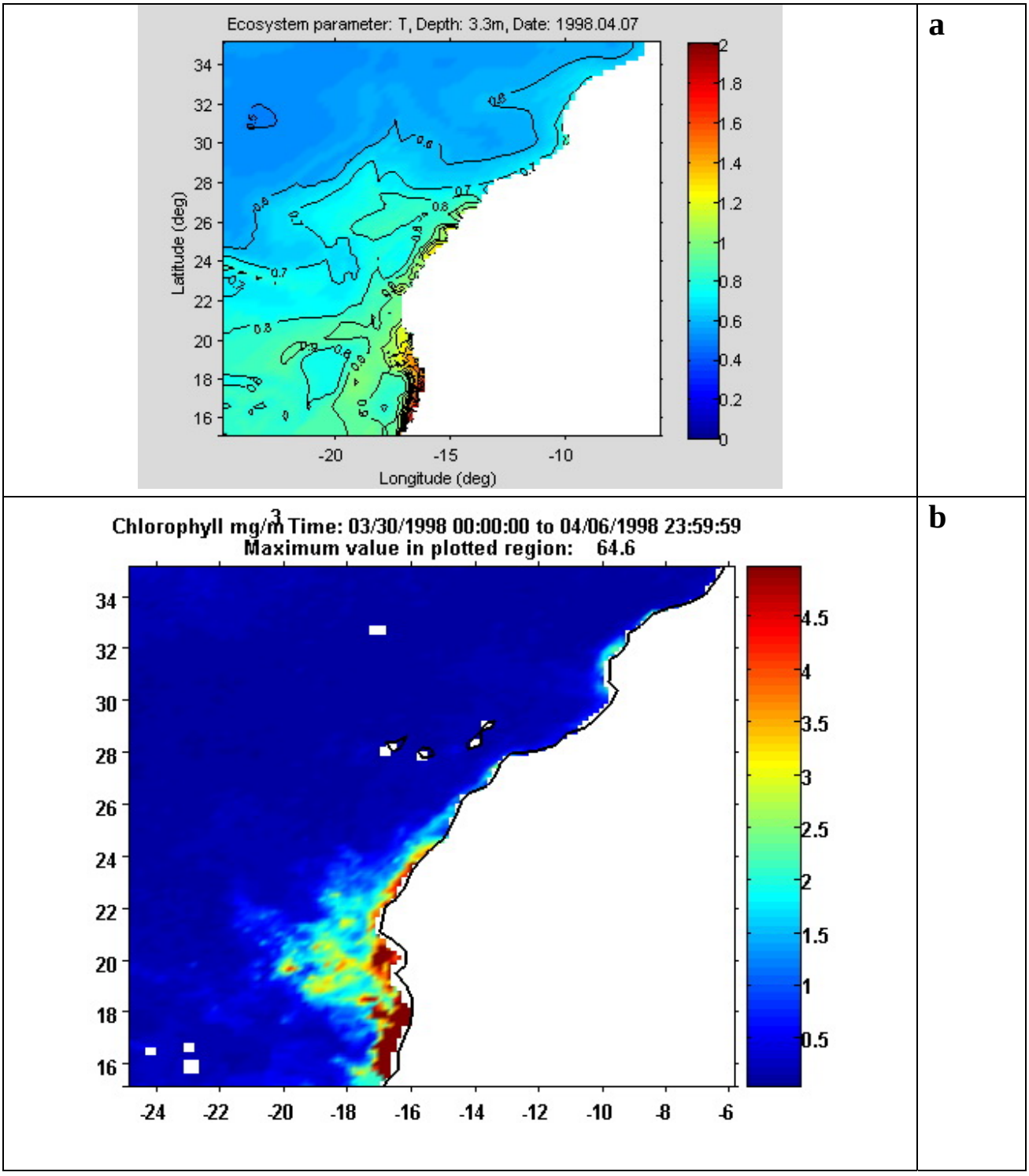

Fig. 12. Sea surface distribution of calculated phytoplankton biomass (mmol N/m^3) on 7 April 1998 (a) and the chlorophyll "a" concentration (mg/m^3) based on SeaWiFS data and averaged over the period 30 March - 6 April 1998. (b).

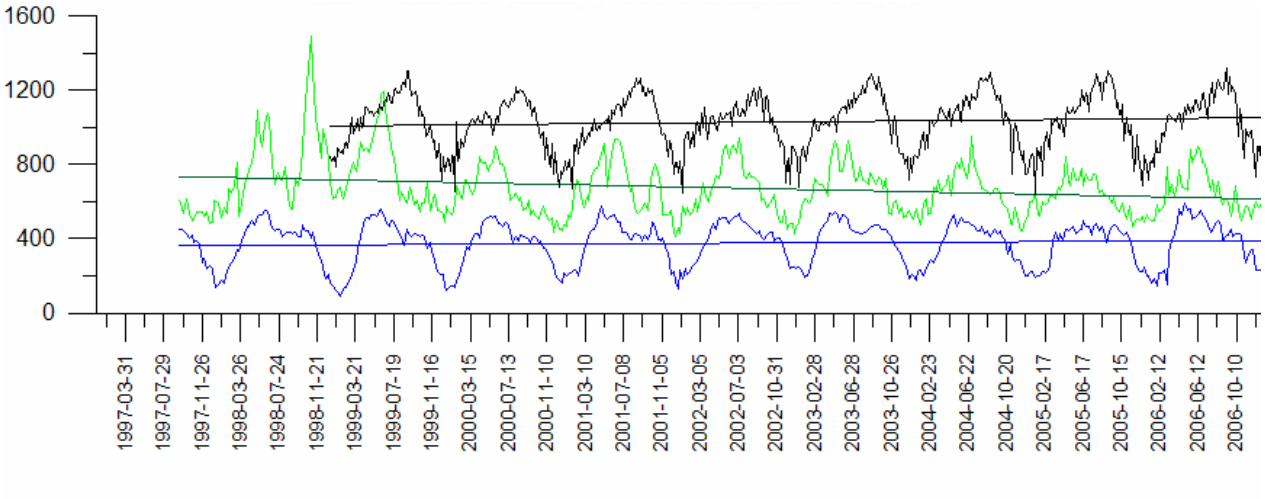

Fig.13. Temporal evolution of area-averaged primary production (mg C/ (m^2 day) in the period from 1998 to 2006. Black curve is the result of model calculations, green and blue lines are satellite-based estimates, respectively, according to the standard Eppley method and carbon method [16].